Exploring the optoelectronic properties of Nitrido-magneso-silicates: Ca[Mg$_3$SiN$_4$], Sr[Mg$_3$SiN$_4$], and Eu[Mg$_3$SiN$_4$]

You may also be interested in:

The mechanical, electronic and optical properties of KH under high pressure: a density functional theory study
An Xinyou, Geng Feng, Ren Weiyi et al.

Systematic study of room-temperature ferromagnetism and the optical response of Zn1xTMxS/Se (TM=Mn, Fe, Co, Ni) ferromagnets: first-principle approach
Q Mahmood, M Hassan and N A Noor

Investigation of structural, mechanical, electronic, optical and dynamical properties of cubic BaLiF3, BaLiH3 and SrLiH3
Battal G Yalcin, Bahadr Salmankurt and Stk Duman

Ab-initio study of the electronic structure and optical properties of KNO3 in the ferroelectric phase
Bahattin Erdinc and Harun Akkus

First principle study of structural stability, electronic structure and optical properties of Ga doped ZnO with different concentrations
H I Berrezoug, A E Merad, M Aillerie et al.

First-principles study of structural, electronic, and optical properties of cubic InAs$_{x}$N$_{y}$P$_{1-x-y}$ triangular quaternary alloys
I Hattabi, A Abdiche, F Soyalp et al.

Exploring the optoelectronic properties of Nitrido-magneso-silicates: Ca[Mg$_3$SiN$_4$], Sr[Mg$_3$SiN$_4$], and Eu[Mg$_3$SiN$_4$]

Sikander Azam[1,2]**, Saleem Ayaz Khan**[1] **and Souraya Goumri-Said**[3]

[1] New Technologies—Research Center, University of West Bohemia, Univerzitni 8, 306 14 Pilsen, Czechia
[2] The University of Lahore, Sargodha Campus, 40100, Pakistan
[3] College of Science, Physics department, Alfaisal University, PO Box 50927, Riyadh 11533, Arabia

E-mail: sosaid@alfaisal.edu

Abstract

Optoelectronic properties of the Nitrido-magneso-silicates Ca[Mg$_3$SiN$_4$], Sr[Mg$_3$SiN$_4$], and Eu[Mg$_3$SiN$_4$] compounds have been investigated using the relativistic full-potential augmented plane-wave method (FLAPW) based on the density functional theory (DFT). The calculations of the electronic and optical properties were conducted by using the local density approximation (LDA), generalized gradient approximation (GGA), and modified Becke Johnson (mBJ) potential. A study of the band structures shows that these compounds are indirect band gap materials. We found a great variation in the obtained energy band gap value as we changed the functionals. The mBJ functional leads to a greater band-gap value compared to LDA and GGA cases. Based on the calculated electronic structure, the optical properties computed, such as the complex dielectric function, absorption coefficient, reflectivity, energy loss function and refractive index, were functions of the photon energy. Origins of the spectral peaks in the optical spectra were discussed and assigned to different electronic transitions observed from the electronic structure calculation.

Keywords: LEDs, phosphors semiconductors, *ab-initio* calculations, electronic structure optical properties

(Some figures may appear in colour only in the online journal)

1. Introduction

Much attention has been paid in order to discover novel materials for light-emitting diodes (LED) devices [1]. Recent studies about white LEDs have shown that their importance that wasn't only limited to energy savings, downsizing, durability and environmental-friendliness, but also in display systems and the next-generation lighting industry. Currently, there is a lot of improvement in white LEDs such as brilliant color-rending properties, high luminous efficacy and high chromatic stability. All these (characteristics) depend on the properties of phosphor that is used to make white LEDs) [2]. Therefore, researchers have focused on white LEDs because of their (i) low cost, (ii) ability to be fabricated easily and (iii) high degree of brightness. In the process, LEDs based on

III–V semiconductors produce a cool white light emission by mixing the blue emission of an InGaN diode chip with the yellow luminescence from Y$_3$Al$_5$O$_{12}$:Ce^{3+} (YAG:Ce^{3+}) phosphor [3]. Oxonitridoaluminosilicates (commonly named oxonitridosilicates) have shown good stability, chemical, thermal and structural diversity [4] to produce LEDs. Those materials are obtained from the oxosilicates by the exchange of oxygen by nitrogen (or silicon by aluminum). Furthermore, by doping the nitridosilicates and oxonitridosilicates with rare elements such as Eu^{2+}, Ce^{3+} (i.e. lanthanide ions), we increased the chances leading to efficient luminescent materials (phosphors), which have significant application (industrial) in white LEDs [5].

In 2014 Sebastian Schmiechen *et al* performed the synthesis and structural characterization of new nitridomagnesosilicates, Sr
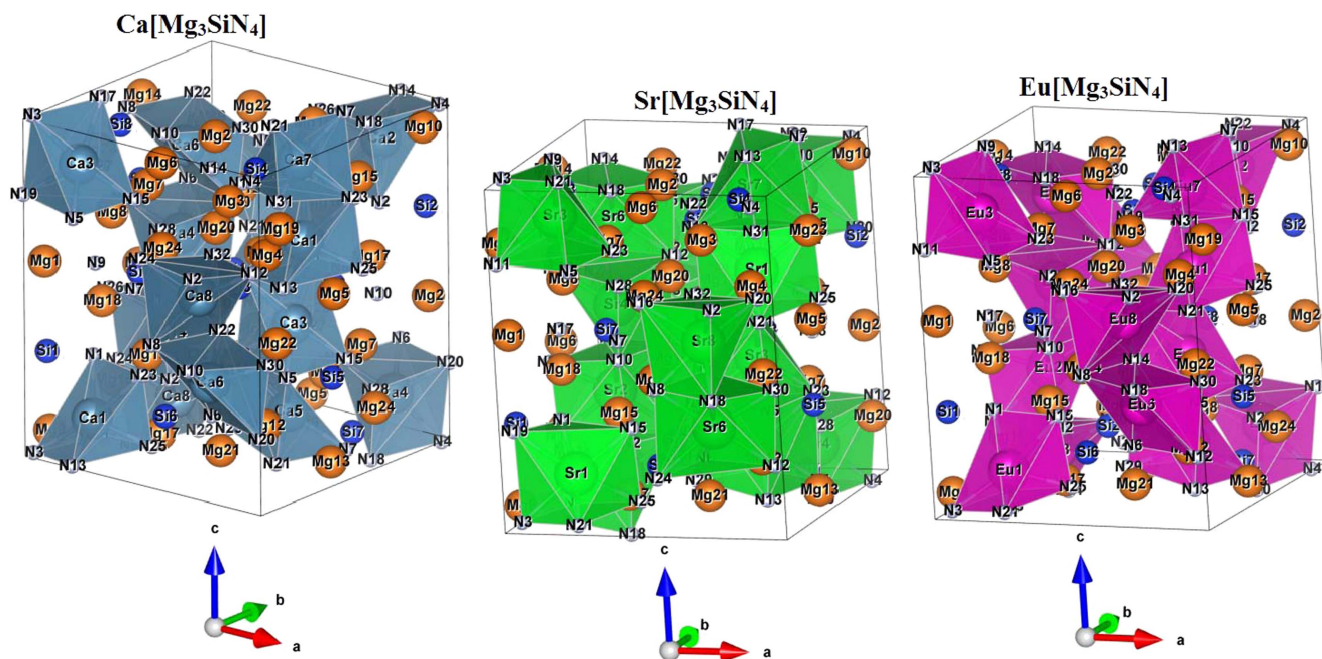
Ca[Mg₃SiN₄] **Sr[Mg₃SiN₄]** **Eu[Mg₃SiN₄]**

Figure 1. Unit cell structure.

[Mg₃SiN₄]:Eu²⁺, Ca[Mg₃SiN₄]:Ce³⁺ and Eu[Mg₃SiN₄]. These materials are promising for LED applications and to date there are no exhaustive theoretical/experimental studies on their electronic structure and optical properties. So, in the present work, we have computationally investigated the electronic and optical properties of X[Mg₃SiN₄] (X = Ca, Sr and Eu) by employing the density functional theory (DFT) to discover their potential use as materials for LED devices. We are using recent approaches developed in *ab-initio* theories that have proved to be a powerful tool for the execution and prediction of theoretical studies of physical/chemical properties of condensed matter. Therefore herein, we carried out an *ab-initio* study of the band structure, density of states, dielectric function (imaginary and real part, other related optical properties like absorption coefficient, reflectivity, energy loss function and refractive index). We used the full potential (linearized) augmented plane wave method with the modified Becke Johnson (mBJ) approximation. The paper has been structured in the following way. In section 2, we describe briefly the computational methodology, in section 3, we discuss the electronic and optical properties of the investigated materials, and finally in section 4 we summarize the present work.

2. Methodology and crystallographic structure

The crystallographic data for the investigated compounds have been considered from the work of Schmiechen *et al* with a symmetry group of $I4_1/a$ (No. 88) [6]. Then, we minimized the forces which act on the atoms. Using this optimized geometry, we carried out a theoretical study of the electronic and optical properties for X[Mg₃SiN₄] (X = Ca, Sr and Eu) compounds. All of these properties were studied using the full potential linearized augmented plane wave as accomplished

in the WIEN2k code [7] based on density functional theory (DFT) [8, 9]. The exchange correlation potential E_{xc} was treated by means of local density approximation (LDA) and generalized gradient approximation (GGA) [10, 11] and modified Becke and Johnson (mBJ) [12–14]. The presence of Europium in Eu[Mg₃SiN₄] led us to consider the +U correction (U Hubbard parameter = 4 eV) that has been shown in earlier studies to describe the *f*-orbitals effectively.

Here, in the present calculations, the number of plane waves have been controlled by setting $R_{MT} \times K_{max} = 7$, whereas $l_{max} = 10$, the wave function expansion in the atomic spheres was controlled with a 13 × 11 × 10 *k*-mesh, which has been tested to reach the convergence criteria. The calculations were performed by fitting the energy convergence at the range of 10^{-4} Ry. The values for muffin-tin radii (R_{MT}) was chosen to be 2.50 a.u. for Eu, 1.53 a.u. for Si, 1.94 a.u. for Mg and 1.78 a.u. for N for Eu[Mg₃SiN₄], 2.4200 a.u. for Sr, 1.4800 a.u. for Si, 1.8200 a.u. for Mg and 1.7200 a.u. for N for Sr[Mg₃SiN₄] and 2.3500 a.u. for Ca, 1.4500 a.u. for Si, 1.8100 a.u. for Mg and 1.6900 a.u. for N for Ca[Mg₃SiN₄]. The crystal structures of the X[Mg₃SiN₄] (X = Ca, Sr and Eu) compounds are presented in figure 1. The lattice parameters for Ca[Mg₃SiN₄] are, *a* = 11.424(2), *c* = 13.445(3) Å; for Sr[Mg₃SiN₄] are, *a* = 11.495(2), *c* = 13.512(3) Å and for Eu[Mg₃SiN₄] are, *a* = 11.511(4), *c* =13.552(4) Å [6].

3. Results and discussion

3.1. Electronic structure

Studying the electronic structure of solid materials is useful in many cases. This does not only predict the chemical/physical properties but also provides insight into various applications;
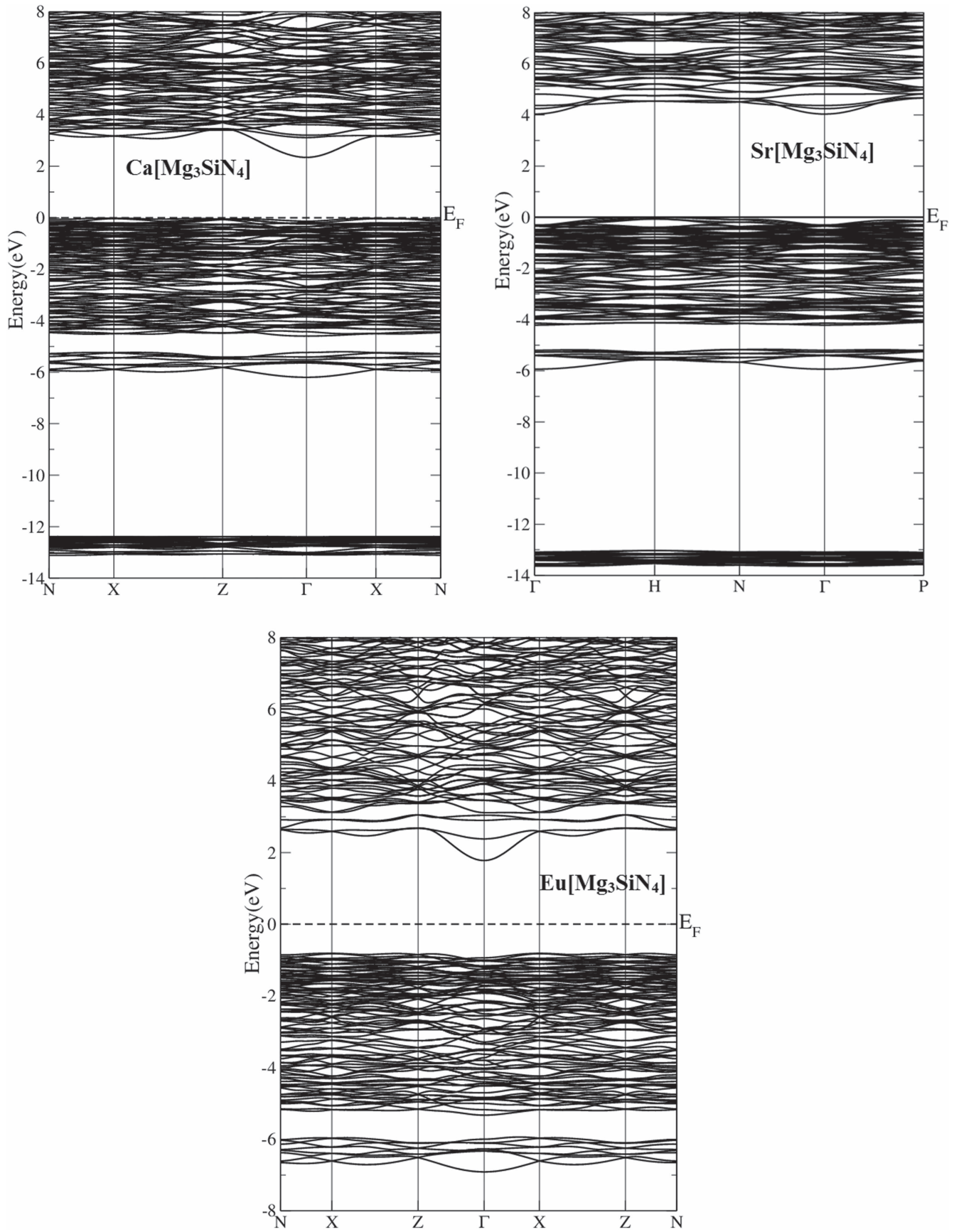
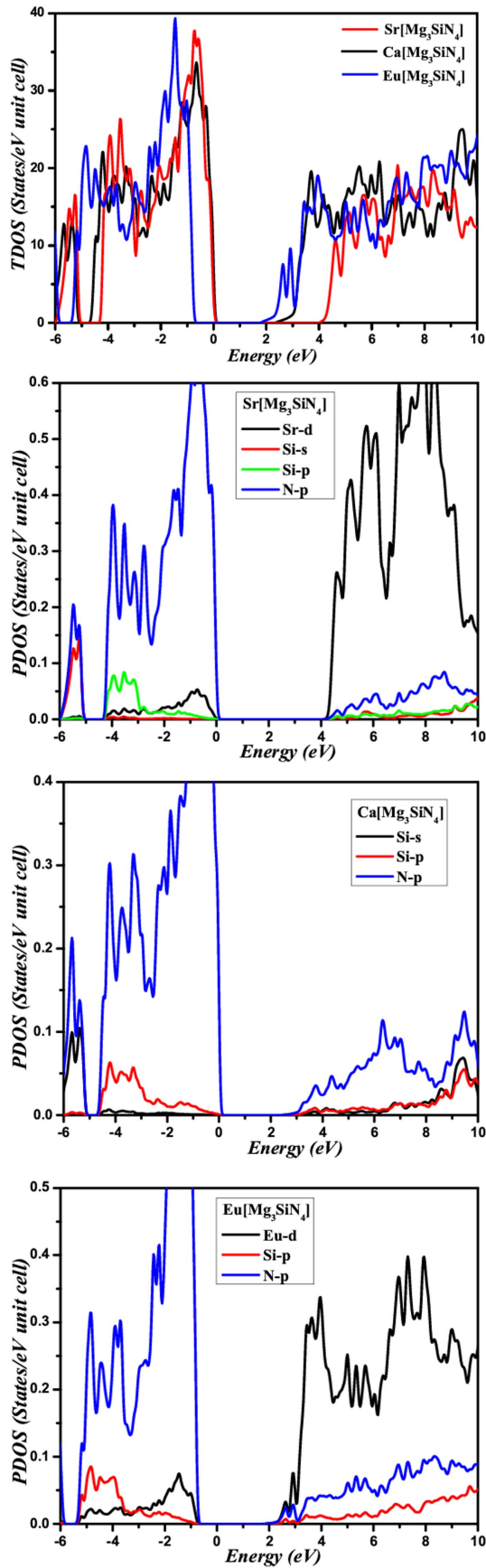**Figure 2.** Calculated band structure.

Figure 3. Calculated total and partial densities of states (States/eV unit cell).

specifically for the understanding of the optical and electronic properties of $X[Mg_3SiN_4]$ (X = Ca, Sr and Eu) where it is useful to examine the electronic band structures. Our calculated energy band structure along the high-symmetry directions has been shown in figure 2, using the mBJ functional. We calculated the band structure using different approximations, i.e., LDA, GGA and mBJ. These approximations show a similar band structure, except for the band gap value which is higher for mBJ.

Our computed electronic structures for the Nitrido-magnesosilicates along the $N \rightarrow X \rightarrow Z \rightarrow \Gamma \rightarrow X \rightarrow N$ for $Ca[Mg_3SiN_4]$ and $Eu[Mg_3SiN_4]$ and $\Gamma \rightarrow H \rightarrow N \rightarrow \Gamma \rightarrow P$ for $Sr[Mg_3SiN_4]$ materials are displayed in figure 2 in the Brillouin zone using the mBJ functional. Our results reveal a band gap of 2.600, 4.226 and 2.596 eV for $Ca[Mg_3SiN_4]$, Sr $[Mg_3SiN_4]$ and $Eu[Mg_3SiN_4]$. For $Ca[Mg_3SiN_4]$ our calculated band gap shows close agreement with the previous result [6]. It is obvious from the band structure spectra that the bands in the $Ca[Mg_3SiN_4]$ and $Sr[Mg_3SiN_4]$ compounds are more dispersive than the $Eu[Mg_3SiN_4]$ compound. The dispersion in the $Ca[Mg_3SiN_4]$ and $Sr[Mg_3SiN_4]$ bands suggest that the holes' and electrons' effective mass will be greater than the $Eu[Mg_3SiN_4]$ compound, but in reflection the mobility of electrons and holes will be smaller in $Ca[Mg_3SiN_4]$ and $Sr[Mg_3SiN_4]$ than the third one. So to understand the orbital character, we scrutinized the density of states. Based on the optimized structures, the band structures along with the total and partial density of states (TDOS and PDOS) of $X[Mg_3SiN_4]$ (X = Ca, Sr and Eu) compounds were plotted in figures 3 and 4, respectively. Primarily, the valence band of $Ca[Mg_3SiN_4]$ is composed of $N-2p^3$ and Si-$2s^2$, $3p^2$ orbitals along with the mixing of Mg-$3s^2$, $2p^6$ orbitals, whereas in the minimum conduction band, the major contribution comes from Sr-$5s^2$ along with Mg-$3s^2$, $2p^6$ orbitals (as shown in figure 3).

3.2. Optical properties

Generally, the optical properties of solids are stated by the physical parameters like the dielectric function (imaginary and real part) and other derived optical constants such as the refractive index, optical conductivity, absorption coefficient, reflectivity etc. In the present work all first-principles-studies based full potential calculations are carried out for ground state properties, that is to say under 0 K. Consequently, the non-equilibrium vibrational excitations and the phonon contributions to the electronic band structure and optical spectra are negligible under or at 0 K and may be ignored.

We can calculate all of these parameters using the frequency-dependent dielectric function $\varepsilon(\omega) = \varepsilon_1(\omega) + i\varepsilon_2(\omega)$ [15, 16], where $\varepsilon_1(\omega)$ and $\varepsilon_2(\omega)$ are the real and imaginary part of the dielectric function. As a direct relation between the electronic structure and dielectric function $\varepsilon(\omega)$ exists, so $\varepsilon(\omega)$ can be obtained from the electronic band structure. Numerically $\varepsilon_2(\omega)$ is evaluated by the matrix elements between the occupied and unoccupied states [17], while the $\varepsilon_1(\omega)$ can be investigated from $\varepsilon_2(\omega)$ using the Kramers–Kronig relation [18–21]. I will mention here that in our
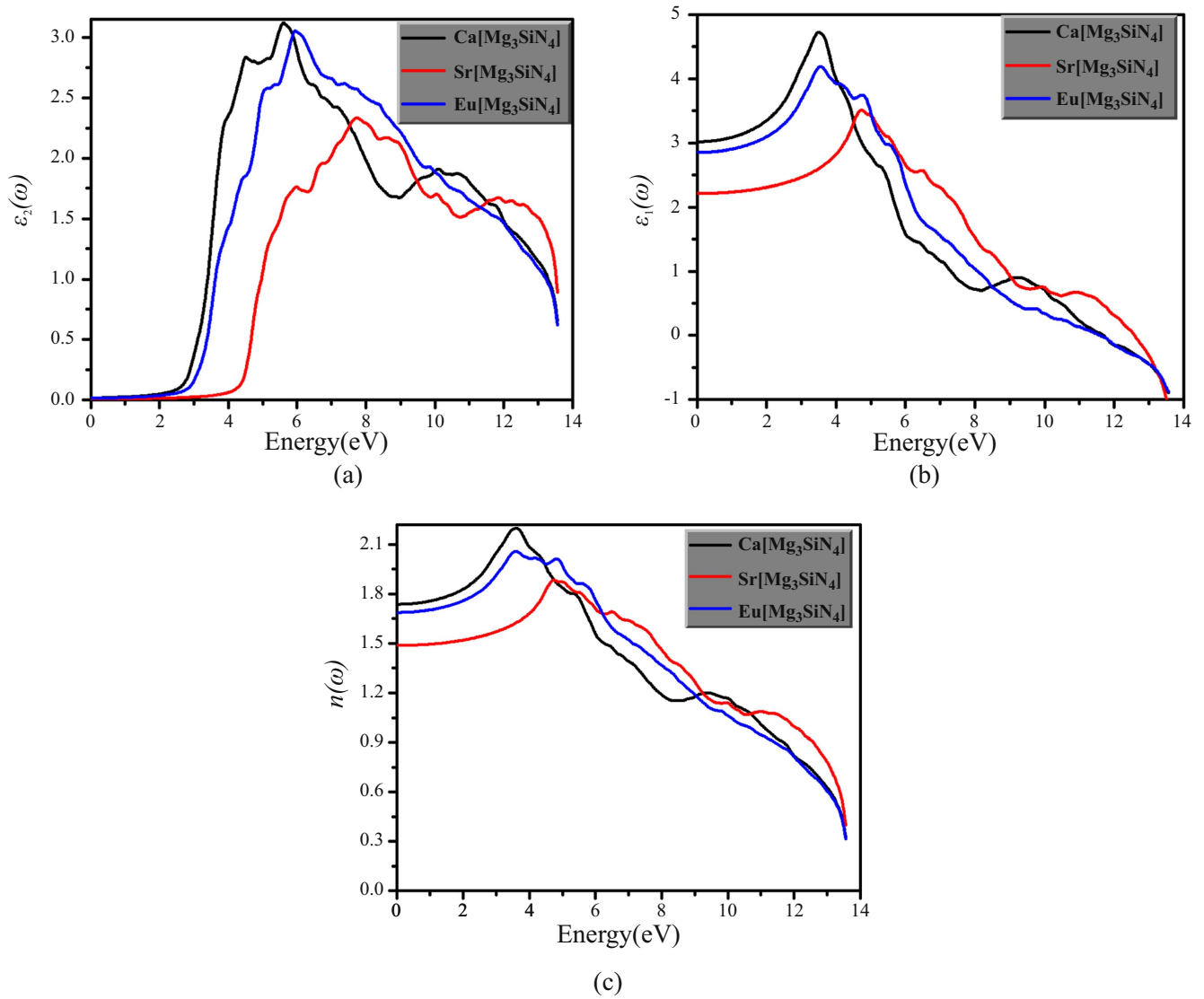
(a)

(b)

(c)

Figure 4. Calculated (a) imaginary $\varepsilon_2(\omega)$, (b) real part $\varepsilon_1(\omega)$ and (c) refractive index $n(\omega)$.

calculations we don't consider the local field effects. For the optical spectra it is important to have the phonon contributions, especially for the indirect band gap material, but we also ignore it here. However, even within these confines our calculated optical spectra shows good agreement with the experimental results [6]. Our calculated average imaginary $\varepsilon_2^{\mathrm{average}}(\omega)$ and real $\varepsilon_1^{\mathrm{average}}(\omega)$ parts of the frequency-dependent dielectric function for the X[Mg$_3$SiN$_4$] (X = Ca, Sr and Eu) are illustrated in the figure 4. As our investigated compounds have tetragonal symmetry and this has two major components (i.e., ($\varepsilon^{xx}(\omega) = \varepsilon^{yy}(\omega)$ and $\varepsilon^{zz}(\omega)$)), here we are dealing with three different compounds, so we will take the average of these two components for each of the materials as shown in figures 4(a) and (b). The threshold (critical point) value for the Ca[Mg$_3$SiN$_4$] is 4.0 eV, as we replace Ca by Sr and Eu the threshold value decreases to 2.3 and 2.2 eV for Sr [Mg$_3$SiN$_4$] and Eu[Mg$_3$SiN$_4$] respectively. Above the critical point region, where we don't have the absorption, the transmission shows in that specific region. This shift of the threshold energy point to lower energies indicates a decrease

in the band gap. The source of this threshold is the transition that occurs from VBM to CBM i.e., $X_V - \Gamma_C$ for Ca [Mg$_3$SiN$_4$] and Eu[Mg$_3$SiN$_4$], and $N_V - \Gamma_C$ for Sr[Mg$_3$SiN$_4$] compounds. This (critical) point is particularly attributed to the electronic transition from the N-2p state of VB to the Si-3p state of CB in Ca[Mg$_3$SiN$_4$], the N-2p state of VB to the Sr-3d state of CB in Sr[Mg$_3$SiN$_4$] and the N-2p state of VB to the Eu-4d state of CB in Eu[Mg$_3$SiN$_4$]. In the literature we didn't find any study related to our results for comparison. Now, here we will state the origin of the transitions that are held responsible for the peaks in the optical spectra. To determine the features and the origin of the peaks of $\varepsilon_2^{\mathrm{average}}(\omega)$ are executed by decomposing it to its individual pair contribution, i.e., $V_i \rightarrow C_j$ (the contribution of each pair in the VB to CB). Generally the major contribution in the optical spectra comes from the VBM to the CBM. The frequency-dependent real part of the $\varepsilon_1^{\mathrm{average}}(\omega)$ and refractive index $n^{\mathrm{average}}(\omega)$ that shows exactly how an electromagnetic energy is dispersed when it perforates in a material as exposed can be seen in figures 4(b) and (c). The $\varepsilon_1^{\mathrm{average}}(\omega)$ (see
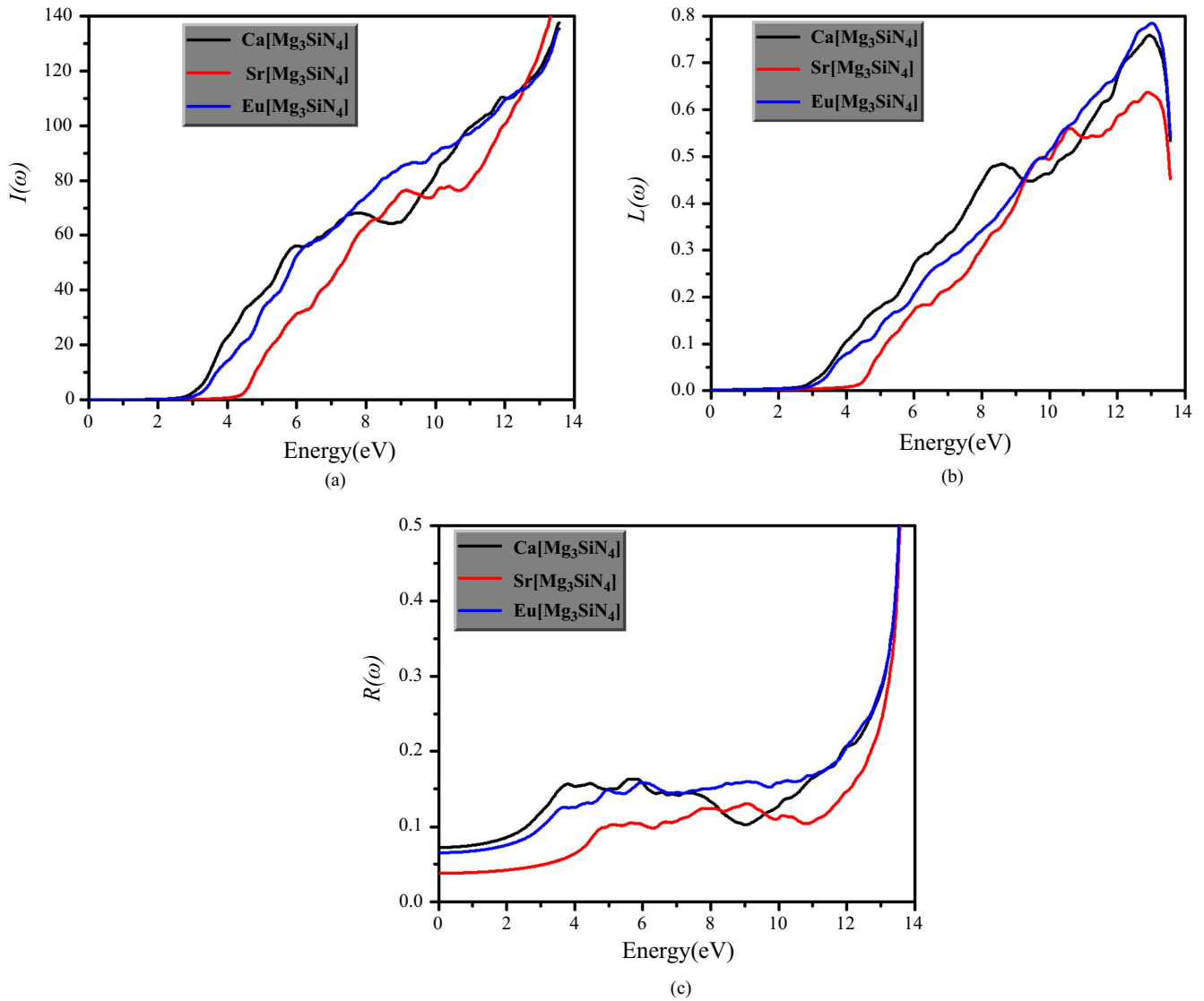
Figure 5. Calculated (a) absorption coefficient $I(\omega)$, (b) energy-loss spectrum $L(\omega)$ and (c) reflectivity $R(\omega)$.

figure 4(b)) curve shows a sharp peak between $4.0 \sim 5.0$ eV and crossing the zero at energy point around 11.0 eV. As the materials cross at the negative energy region they behave metallic in nature. The static dielectric constant $\varepsilon_1^{\text{average}}(0)$ at the zero energy limit are 3.0, 2.7 and 2.2 for Ca[Mg$_3$SiN$_4$], Sr[Mg$_3$SiN$_4$] and Eu[Mg$_3$SiN$_4$]. One can see that with the increasing energy gap the values of $\varepsilon_1^{\text{average}}(0)$ decrease which can be explained by the Penn model [22]. The expression for the Penn model is given below

$$\varepsilon_1(0) \approx 1 + (\hbar\omega_p/E_g)^2$$

This shows that $\varepsilon_1(0)$ has an inverse relation with E_g. If one knows the values for $\varepsilon_1(0)$ and $\hbar\omega_p$ then it's easy to calculate E_g. The values for the static refractive index $n(0)$ (see figure 4(c)) are 1.75, 1.60 and 1.50 for X[Mg$_3$SiN$_4$] (X = Ca, Sr and Eu). One can see this with the increasing energy in the visible region and reaching the maximum peak in the near ultraviolet at about 3.5 eV. These higher values suggest that the present materials can be operated magnificently for photonic applications. Beyond this energy point it then decreases and crosses the unity at

10.0 eV and goes to the minimum at higher energy. In the area where it goes down and crosses the unity, for the wave packet the group velocity goes up above the light velocity in free space, that leads to the assumption that these materials show superluminal behavior within this energy range. In the DFT study the superluminal behavior is not surprising because of the Kramers–Kronig equation [18–21] that is based on electromagnetic (EM) responses, yielding such output for almost every material at some specific spectral range of EM waves and does not break any physical law.

Understanding of $n(\omega)$ is important for devices like solar cells, wave guides, photonic crystals, detectors and so on. The reflectivity coefficient $R(\omega)$ (see figure 5(c)), energy loss function $L(\omega)$ (see figure 5(b)) and absorption coefficient $I(\omega)$ (see figure 5(a)) show different ways to report how the EM (electromagnetic) energy is taken as this interacts with a material as displaced in figure 5(a). For the photoelectric materials, one of the important factors to evaluate is the optical absorption coefficient $I(\omega)$. Our calculation shows that the absorption coefficient spectra show that the investigated materials have good

optical absorption at a higher energy range. As we can see, these compounds can absorb in all of the energy regions that exist in UV (ultraviolet) light. Consequently, these materials may be used as a filter for energies in the far UV spectrum. The values that are obtained for the investigated compounds in our calculations for $R(\omega)$ don't increase more than 20%, up to 12.0 eV (see figure 5(c)). This shows that these compounds behave like semiconductors. The reflectivity of the calculated compounds reaches a maximum value of 50%. The behavior of the reflectivity spectra marks these materials as worthy for applications in the VIS and UV region. Our computed energy-loss function $L(\omega)$ is presented in figure 5(b), which is one of the significant factors that state the energy loss of a fast electron passing through the material. The peaks in the $L(\omega)$ spectra signifying the characteristic that is related to the plasma resonance is known as the plasma frequency up. The most noteworthy phenomena that occur here is the descending of the spectral peaks in the reflectivity spectra at a specific energy point in accord with a strong peak in the $L(\omega)$ spectra on account of the collective plasma resonance. The peaks in the electron-energy loss are consistent with the decreasing edges in the $R(\omega)$ (see figure 5(c)) spectra, such as the maximum booming $R(\omega)$ at 14.0 eV for three materials corresponding to the abrupt reduction in electron–energy loss spectra.

4. Conclusions

We employed the *ab-initio* FP-LAPW method to scrutinize the electronic and optical properties of the $X[Mg_3SiN_4]$ (X = Ca, Sr and Eu) using different approximations LDA and GGA. But to accurately report the electronic structure (band structure and density of states), we used the modified Becke Johnson (mBJ) functional to the exchange–correlation potential term. The band structure shows semiconductor behavior with an indirect band gap for all investigated compounds. Furthermore, compared to the other (old) functional, the mbJ has successfully reproduced the experimental band gap. We explored the energy dependent dielectric function imaginary and real part together with a complete set of the related optical constants, like the absorption coefficient, energy loss function, reflectivity coefficient, and refractive index. We found an inverse relation between the values of $\varepsilon_1(0)$ and energy band gap that was explained using the Penn model. The optical properties show that the studied Nitridomagneso-silicates materials could exhibit interesting applications in the visible and ultraviolet region.

References

[1] Azam S *et al* 2015 *Curr. Appl. Phys.* **15** 1160e1167
[2] Zhang C, Uchikoshi T, Xie R-J, Liu L, Cho Y, Sakka Y, Hirosaki N and Sekiguchi T 2015 *J. Mater. Chem.* C **3** 7642–51
[3] Luong V D, Zhang W and Lee H-R 2011 *J. Alloys Compd.* **509** 7525–8
[4] Xie R-J, Hirosaki N, Suehiro T, Xu F-F and Mitomo M 2006 *Chem. Mater.* **18** 5578–83
[5] Zeuner M, Schmidt P J and Schnick W 2009 *Chem. Mater.* **21** 2467–73
[6] Schmiechen S, Schneider H, Wagatha P, Hecht C, Schmidt P J and Schnick W 2014 *Chem. Mater.* **26** 2712−9
[7] Blaha P, Schwarz K and Luitz J 1999 WIEN97, A Full Potential Linearized Augmented Plane Wave Package for Calculating Crystal Properties, Karlheinz Schwarz, Techn. Universit at Wien, Austria, ISBN3-9501031-0-4
[8] Hohenberg P and Kohn W 1964 Inhomogeneous electron gas *Phys. Rev.* **136** B864
[9] Kohn W and Shom L J 1965 Self-consistent equations including exchange and correla-tion effects *Phys. Rev.* **140** A1133
[10] Ceperley D M and Alder B J *Phys. Rev. Lett.* **45** 566–9
[11] Perdew J P, Burke K and Ernzerhof M 1996 Generalized gradient approximation madesimple *Phys. Rev. Lett.* **77** 3865
[12] Becke A D and Johnson E R 2006 *J. Chem. Phys.* **124** 221101
[13] Tran F and Blaha P 2009 *Phys. Rev. Lett.* **102** 226401
[14] Tran F, Blaha P and Schwarz K 2007 *J. Phys.: Condens. Matter* **19** 196208
[15] Azam S *et al* 2015 *Mater. Res. Bull.* **70** 847–55
[16] Azam S *et al* 2015 *J. Solid State Chem.* **229** 260–5
[17] Amrosch-Draxl C and Sofo J O 2006 *Comput. Phys. Commun.* **175** 1
[18] de L Kronig R 1926 On the theory of the dispersion of x-rays *J. Opt. Soc. Am.* **12** 547
[19] Kramers H A 1927 La diffusion de la lumiere par les atomes *J. Atti Cong. Intern. Fisica (Trans. Volta Cent. Congress) Como* **2** 545
[20] Jackson J D 1975 *Classical Electrodynamics* (New York: Wiley)
[21] Bohren C F 2010 *Eur. J. Phys.* **31** 573
[22] Penn D R 1962 *Phys. Rev.* **128** 2093–7